Saponite-anthocyanin derivatives: The role of organoclays in pigment photostability

Luciano C.B. Lima, Fabrícia C Silva, Edson C Silva-Filho, Maria G Fonseca, Guanzheng Zhuang, Maguy Jaber

Saponite-anthocyanin derivatives: The role of organo-clays in pigment photostability

Luciano C. B. Lima[1,2], *Fabrícia C. Silva*[1,2], *Edson C. Silva-Filho*[2], *Maria G. Fonseca*[3], *Guanzheng Zhuang*[4,5], *Maguy Jaber*[1]*

[1]Sorbonne Université, CNRS UMR 8220, LAMS, Institut Universitaire de France (IUF), case courrier 225, 4 pl. Jussieu 75252 Paris cedex 05, France

[2]LIMAV, Univ. Federal do Piauí – UFPI, 64049-550 Piauí, Brazil

[3]NPE-LACOM, Univ. Federal da Paraíba – UFPB, João Pessoa, 58051-900 Paraíba, Brazil

[4] CAS Key Laboratory of Mineralogy and Metallogeny, Guangzhou Institute of Geochemistry, Chinese Academy of Sciences, Guangzhou 510640, China.

[5] Guangdong Provincial Key Laboratory of Mineral Physics and Materials, Guangzhou 510640, China.

AUTHOR INFORMATION

Corresponding Author

*Tel: +33-(0)1-4427-6289

*Email: maguy.jaber@sorbonne-universite.fr

ABSTRACT

Hybrid pigments based on organo-saponite (cetyltrimethyl ammonium bromide (CTAB-Sap) and a commercial anthocyanin (ACN) dye, Crystal Red Grape, were prepared. The interactions between organic dye guest and hosts (including saponite and organo-saponite) were investigated by X-ray diffraction, transmission electron microscopy and Fourier transform infrared spectroscopy. The pigments exhibit different colors function of their host-guest interactions. The blue color of organo-clay-anthocyanin indicates the stabilization of quinoidal base form of the dye. The hybrids have good stability against visible light irradiation and basic pH conditions. These dyed materials are environmentally friendly and can be promising candidates in different application fields.

Keywords: organo-saponite, anthocyanin, photostability, chemical stability

GRAPHICAL ABSTRACT

-

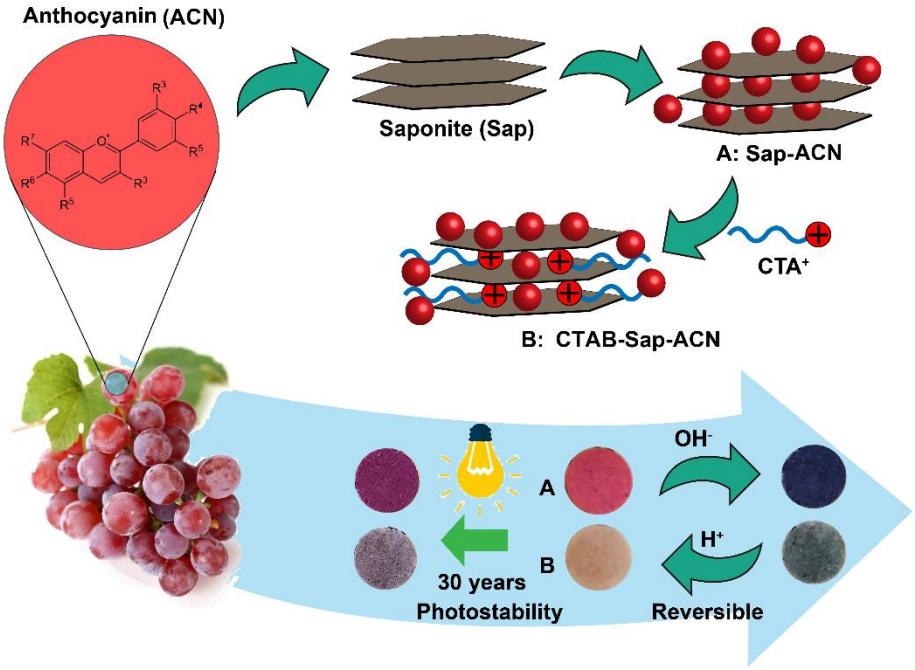

KEYWORDS: Saponite, Organo-functionalization, Natural dye, hybrid pigment, Color change.

1. Introduction

The increasing awareness of consumers regarding food safety has been leading the preference for natural dyes instead of synthetic ones. Anthocyanins (ACN) have an antioxidant and free-radical scavenging properties that make them attractive as substitutes of synthetic dyes. These natural dyes have the 7-hydroxyflavylium cation chromophoric group in their structure which is responsible for most of the purple, blue and red colors of flowers and fruits (Brouillard, 1982; Fang et al., 2020). In spite of their potential use in several fields, anthocyanins have limitations due to their photo- and chemical-stabilities (Torres et al., 2011; Silva et al., 2018). Anthocyanin dyes are unstable to external environmental conditions such as light, pH, oxygen, temperature (Piffaut et al., 1994).

Therefore, biohybrid compounds that combine these biomolecules and an inorganic substrates such as clay minerals have been widely investigated to reverse these limitations by interaction/protection in the host materials (Kohno et al., 2009; Teixeira-Neto et al., 2012; Pimchan et al., 2014; Lu et al., 2019; Samuei et al., 2020).

This strategy is inspired by Maya Blue pigments, in which a variety of clay minerals and organic dyes have been used to prepare stable pigments (Trigueiro et al., 2018; Chen et al., 2019; Zhuang et al., 2019a; Silva et al., 2020). Concerning the ACN stabilization, montmorillonite, synthetic non-swelling mica and silica were employed by Kohno et al., 2009 to improve the stability of ACN against alkaline environment and visible light irradiation. In their study, the best results were obtained by ACN intercalation into montmorillonite. Electrostatic interactions between the intercalated dye and the montmorillonite surface were highlighted and the intercalation protected the dye from atmospheric oxygen (Kohno et al., 2009). Li et al., 2019 have reported the acid/base reversible allochroic hybrid pigments prepared by incorporation of

ACN on sepiolite, halloysite, kaolinite and montmorillonite. Their comparative study has demonstrated the influence of the clay compositions on color properties, the nanochannels of Sep were claimed to be responsible for the optimum vivid color properties, thermal stability, and chemical corrosion resistance (Li et al., 2019b). Palygorskite was also studied to provide enhancement in ACN stability (Li et al., 2019a).

Functionalized clays have also attracted broad attention in the field of lake pigments since they provide better chemical and thermal stability. Recent studies have improved the clay properties by pillaring process (Trigueiro et al., 2018), organo-functionalization with aminosilane (De Queiroga et al., 2019) as well as incorporating a variety of surfactants (Wang and Wang, 2008; Baez et al., 2009; Micó-Vicent et al., 2017). In addition, our group recently reported hybrid pigments with excellent stability by incorporation of alizarin with a variety of organo-modified clays with cetyltrimethylammonium bromide (CTAB) (Silva et al., 2020), Rhodamine 640 perchlorate, sulforhodamine B and Kiton red 620 (Tangaraj et al., 2017) dyes. Despite of the wide use of modified clays to enhance the stabilities of organic dyes, no study explored the stability enhancement for anthocyanin after adsorption on modified clay.

This work describes the hybrid pigments formation by adsorption of anthocyanin on saponite (Sap) and an organic modified saponite with cetyltrimethylammonium bromide (CTAB-Sap). These pigments were characterized and their photo- and chemical- stabilities were evaluated.

2. Materials and methods

2.1. Materials

Anthocyanin (ACN) source was a Crystal Red Grape (90%, wt) donated by San Joaquin Valley Concentrates (Fresno, CA, USA). cetyltrimethylammonium bromide (CTAB) (99%, wt), citric acid (99.5 %, wt), sodium citrate (99 %, wt), sodium hydroxide (98 %, wt), hydrochloric acid, and other applied chemicals were purchased from Aldrich or Sigma-Aldrich, all with an analytical grade and used without any previous purification.

2.2. CTAB-Saponite preparation procedure

2 g of cetyltrimethylammonium bromide (CTAB) were dissolved in 10 mL of 1 mol L^{-1} HCl solution and added dropwise at room temperature to the stirred aqueous suspension of Na-Sap (previously prepared by us (Jaber and Miéhé-Brendlé, 2005; Tangaraj et al., 2017). After continuous stirring the mixture at 400 rpm for 3 h, the white precipitate was collected by centrifugation, washed with water until no bromide ion could be detected by an aqueous $AgNO_3$ solution, and then dried at 60°C for 24 h.

2.3. Hybrid pigments preparation procedure

1 g of Na-Sap or CTAB-Sap were dispersed in 100 mL of anthocyanin (ACN sample donated by San Joaquin Valley Concentrates (Fresno, CA, USA)) citric acid buffer solution at pH 3 (the ACN concentration was 100 mg L^{-1}) and was stirred at 400 rpm for 1 h. The samples were then centrifuged and dried at 50°C overnight. The hybrid pigments samples are named Sap/ACN and CTAB-Sap/ACN.

2.4. Characterizations

X-ray diffraction were recorded using D8 Advance Bruker-AXS Powder X-ray diffractometer with CuKα radiation (λ = 1.5405 Å). Infrared analyzes were performed on Agilent Cary 630 FTIR spectrometer using an Agilent diamond Attenuated Total Reflectance (ATR) technique mode. Thermogravimetric analyses were carried out using a TA Instrument SDT Q600 analyzer. The heating rate was of 5°C min^{-1} from 25°C to 1000°C, air flow of 10 mL • min^{-1}, and using alumina pan. TEM study of the samples was performed on a JEOL 2010 microscope, 200 kV LaB6 coupled Orius camera, from Gatan Company.

2.5. Chemical stability and photostability

Exposure of the hybrid pigments to basic and acidic conditions in a desiccator containing aqueous NH_4OH or HCl to saturate the atmosphere with HCl or NH_3 vapors was carried out, sequentially and repeatedly (Ogawa et al., 2017).

The pigments were exposure to white light irradiation for 192 h, using a LED lamp set to provide 100 Klux of illumination intensity, in which this time is equivalent to approximately 32 years of exposure in ambient light conditions (Zhuang et al., 2019a, 2019b). The pressed pigments (into pellets) were placed in a desiccator filled with air or nitrogen. The absorbance, reflectance and CIE (Commission Internationale de L'Eclairage) parameters were obtained from an Ocean Optics Halogen and Deuterium Light Source HL-2000-FHSA device as incident light beam and ocean optics USB4000 detector for acquisition. Ocean Optics QP400-1-UV-VIS fiberglass was used to link these devices.

The diffuse reflectance (R) converted into equivalent absorption coefficient F(R) using Kubelka–Munk equation (Eq. (1)) (Silva et al., 2018).

$$F(R) = \frac{(1-R)^2}{2R} \quad (1)$$

The "Commission Internationale of l'Eclairage" CIE 1976 color space system was applied to evaluate the color of the pigments. Measurements were done on pressed pellets samples as function of L^*, a^* and b^* coordinates. The parameter Lightness (L^*) represents the brightness (+) or darkness (−) of the color, i.e., more positive L^* values refer to whiter while more negative L^* values represent darker. While, the values of a^* and b^* indicate the color details: $+a^*$ is the red direction, $-a^*$ the green direction, $+b^*$ the yellow direction, and $-b^*$ the blue direction (Zhuang et al., 2019b). The differences of colors between unexposed and exposed samples were calculated by $\sqrt{((\Delta L^*)^2 + (\Delta a^*)^2 + (\Delta b^*)^2)}$ equation.

3. Results and Discussion

The XRD pattern of the sodium saponite (Fig. 1A) showed the (001) reflection at 7.66° (2θ), corresponding to the basal spacing of 1.16 nm. After organic modification with CTAB, the basal spacing increased to 1.62 nm in CTAB-Sap. This phenomenon indicates that CTA^+ cations successfully intercalated into the interlayer space of Sap by cation exchange with Na^+. The difference between the Sap layer thickness (0.96 nm) and the basal spacing of CTAB-Sap (1.62 nm) was 0.66 nm, which is consistent with a monolayer arrangement of the organic molecules considering the dimensions of CTA^+ cations (at about 0.51 nm) (Marçal et al., 2015).

After loading with anthocyanin, the (001) reflection of Sap/ACN was broader, however, no significant change was observed in the $d_{(001)}$ values of CTAB-Sap/ACN suggesting a surface (or edge) loading

TEM micrographs showed layers with alternate dark and bright fringes allowing the measurement of interplanar distances. For Na-Sap, an interlayer distance of 1.19±0.11 nm was obtained (Figure 1B). In CTAB-Sap, the interlayer distance increased to 1.57±0.19 nm (Figure 1C). After loading with anthocyanin molecules, the $d_{(001)}$ spacing were 1.39±0.19, 1.49±0.20 nm for Sap/An, CTAB-Sap/ACN, respectively (Figure 1 D and E) and some exfoliated layers were observed corroborating with the enlargement of the (001) reflection observed in XRD.

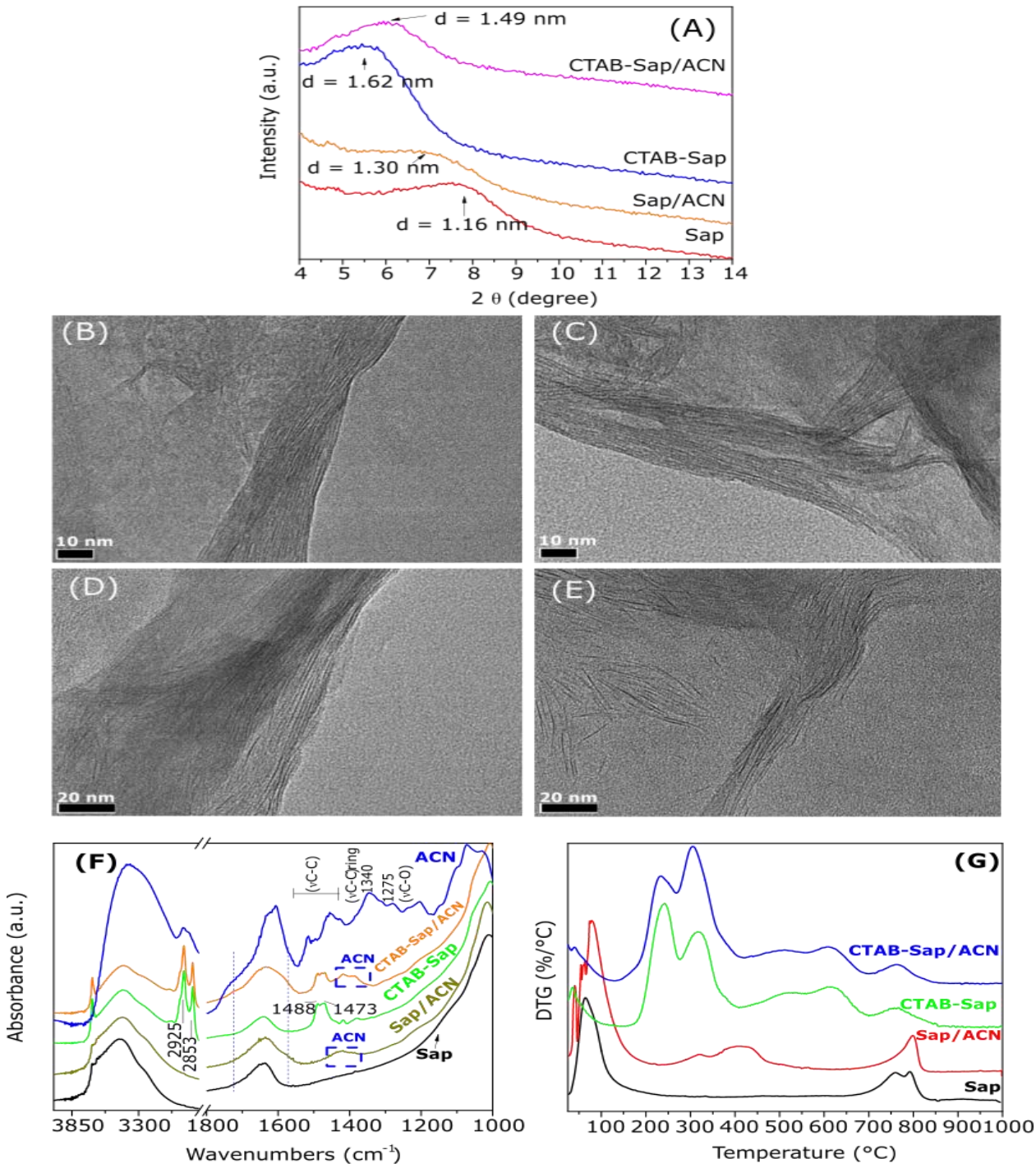

Figure 1. (A) XRD patterns of Sap, Sap/ACN, CTAB-Sap and CTAB-Sap/ACN; TEM images of (B) Sap, (C) Sap/ACN, (D) CTAB-Sap and (E) CTAB-Sap/ACN; (F) FTIR spectra of Sap, Sap/ACN, CTAB-Sap, CTAB-Sap/ACN and (G) DTG curve of Sap, Sap/ACN, CTAB-Sap and CTAB-Sap/ACN.

The FTIR spectra are depicted in Fig.1. For Sap, the sharp and weak band at 3677 cm^{-1} and the one between 3000-3600 cm^{-1} correspond to the stretching vibration of structural –OH group and adsorbed water, respectively. The band at 1633 cm^{-1} is attributed to the bending vibration of –OH. The band at 980 cm^{-1} was assigned to the Si-O-Si stretching (Tao et al., 2016; Fatimah et al., 2019). Several new bands at 2925, 2853, 1488 and 1473 cm^{-1}, which were assigned to the characteristic vibrations of CTAB alkyl chain, emerged in the FTIR spectrum of CTAB-Sap, demonstrating the presence of organic molecules. Concerning the Sap/ACN and CTAB-Sap/ACN samples, the contributions of OH and C=O modes brought from loaded ACN as well as the new hydrogen bond formed in the hybrid pigments make the bands at the regions between 3000-3760-cm^{-1} and 1550-1760 cm^{-1} broader than the respective precursor. The signals in the region between 1350-1470 cm^{-1} are attributed to the contribution of ν(C-C) in aromatic ring of anthocyanin loaded.

In Figure 1G, the first step of mass loss (8%) at 25-238°C for Na-SAP was assigned to the dehydration of surface and interlayer water. The second event at 640-859°C is due to dehydroxylation of Sap with a mass loss of 3% (Tangaraj et al., 2017; Zhang et al., 2017). The DTG curve of Sap/ACN shows an additional mass loss of 7% in the region 210-623°C attributed to the degradation of the incorporated anthocyanin. The mass loss in the second event of CTAB-Sap sample before the ACN adsorption was 30%. After dye loading, the organic mass loss increases to 32% for CTAB-Sap/ACN sample.

The hybrid pigments were exposed to HCl or NH_3 saturated atmosphere. The results upon exposure to acidic and basic vapors were monitored by visible absorption spectroscopy and also by visual changes in their photographs, these results are present in Figure 2.

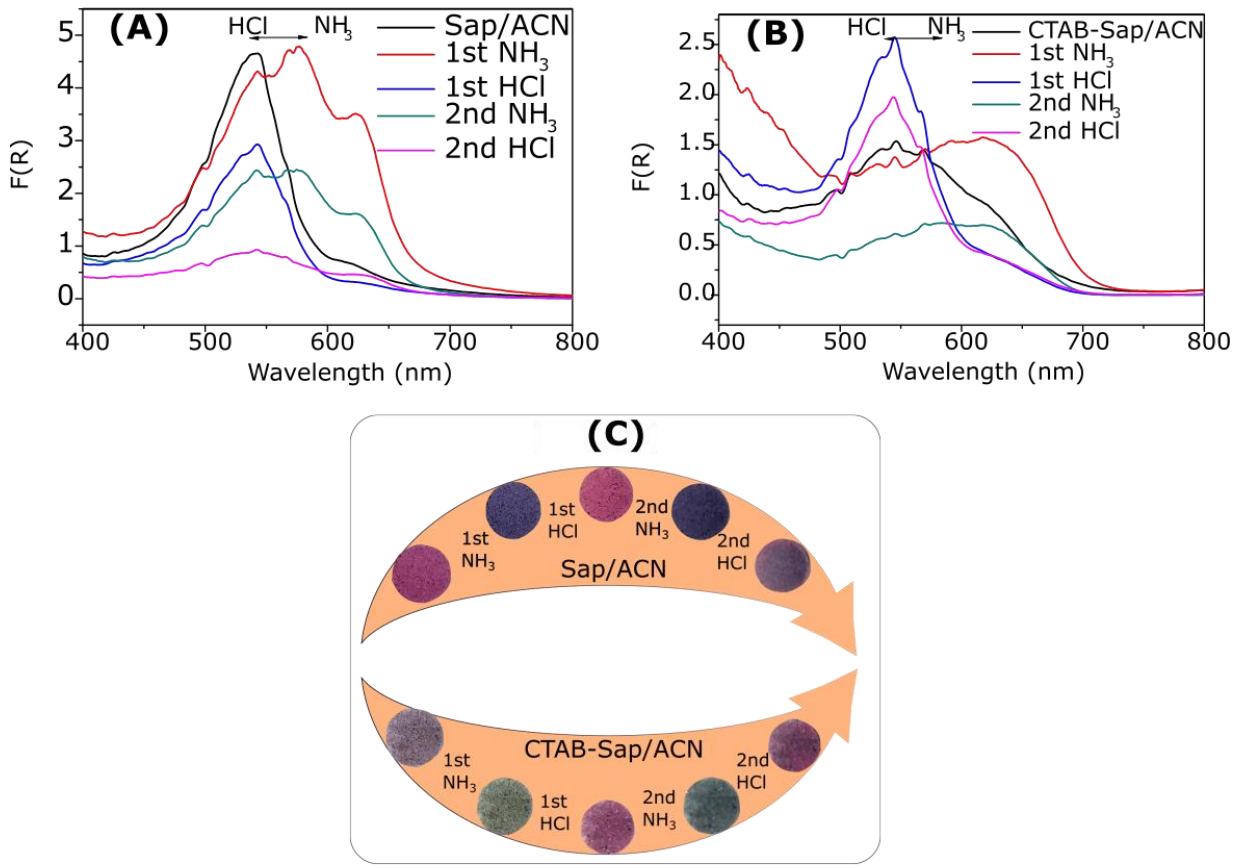

197

198 **Figure 2.** Spectra changes after each step of sequential exposure to acidic and basic atmosphere
199 for (A) Sap/ACN; (B) CTAB-Sap/ACN. (C) Digital photographs of the color changes of hybrid
200 pigments upon exposure.

201 Colors changes from red to blue after exposure to basic atmosphere (NH_3 from aqueous
202 NH_4OH) were observed in the Sap/ACN. The process is reversible, as shown in Figure 2C. The
203 exposure time to change the color was about 10 min. Similar results were obtained in the
204 literature.

205 In Figure 2A, the absorption band has a redshift after exposure to basic atmosphere, and
206 return to the same wavenumber, after exposure to basic atmosphere. After several cycles; the
207 same observations on the spectra were noticed. The color change was reversible and repeatable

for at least two cycles. The color changes are still observed after the second cycle of exposure, although strong acid and base conditions degraded the pigments.

The contribution of quinoidal base in the anthocyanin molecule in CTAB-Sap/ACN was more pronounced than in the other hybrid and explains its initial blue color. After the first exposure to basic vapor, the right shift observed in Figure 3B is due to the conversion of remaining flavylium cations to quinoidal base, which causes a change only in nuance of blue (Figure 2C). Hybrids being exposed to basic conditions were again submitted to acidic environment, the color of CTAB-Sap/ACN change to red and their spectra were similar to the Sap/ACN, indicating that the anthocyanin molecules became flavylium cation form. The behavior of color change in the following cycles was also similar to the Sap/ACN (Ogawa et al., 2017; Silva et al., 2018; Eskandarabadi et al., 2019; Koosha and Hamedi, 2019). The decreases in relative absorbance after the end of four cycles are 80.4% and 73.8% for Sap/ACN, CTAB-Sap/ACN, indicating a slightly better chemical stability for CTAB-Sap/ACN.

The colors of solid hybrid pigments were evaluated before and after light exposure during 192 h (32 years of exposure in a museum). Measurements of $L^*a^*b^*$ parameters were carried out at different light irradiation time (Figure 3).

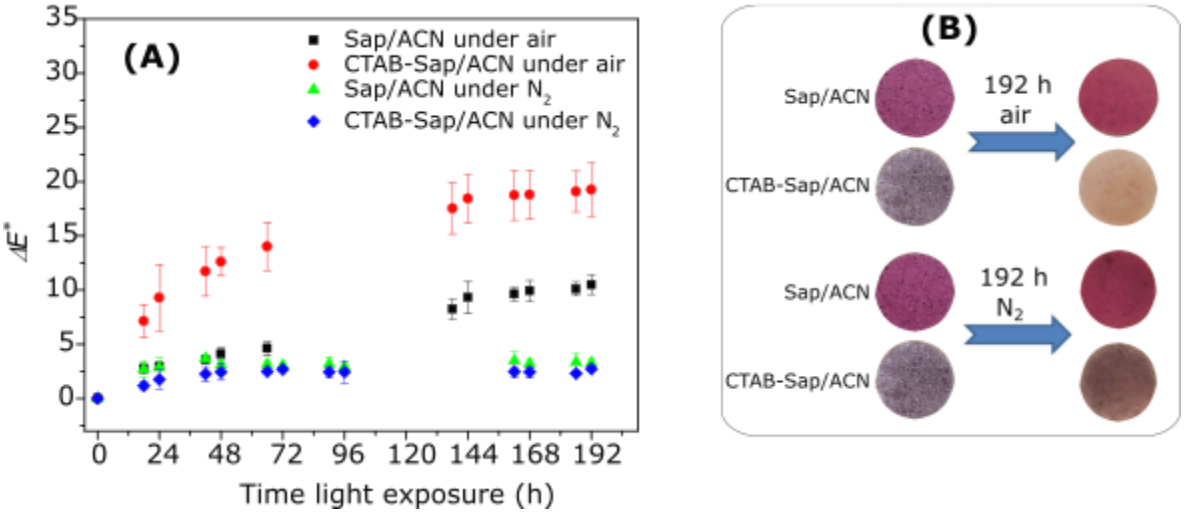

225

226 **Figure 3.** (A) Photo-ageing of pigments and (B) digital photographs of color change
227 observations over 192 h of light exposure in air and nitrogen atmosphere.

228 In solution, the color of ACN changes from red in acid conditions to blue in neutral to
229 weak alkaline conditions. However, the difference in color presented by the hybrids results from
230 the different interactions between the host and the guest since the effect of pH on the color was
231 controlled with the citric acid buffer solution. The color for Sap/ACN is probably due to the
232 intercalation of ACN molecule in the interlayer space of Sap, which stabilizes the red color of
233 flavylium cations. While adsorption in the CTAB-Sap/ACN sample probably induced
234 stabilization of the ACN quinoidal base, leading to a blue color for the hybrid.

235 The ΔE^* value (Figure 3A) is related to total color difference and is indicative of the light
236 stability of the pigments. Under air, the ΔE^* values of the pigments increased gradually with the
237 increase of the ageing time. Finally, the values reached 10.5±0.9 for Sap/ACN and 19.3±2.5 for
238 CTAB-Sap/ACN after 192 h of light exposure. Lower ΔE^* variation in Sap/ACN is probably due
239 to the protection of the dye in the interlayer space of the saponite, creating an oxygen hindering
240 and stabilizing the pigments under irradiation. In nitrogen atmosphere, ΔE^* values were lower
241 after 192 h of light exposure, the ΔE^* values were 2.7±0.2 and 3.3±0.2 for CTAB-Sap/ACN and

Sap/ACN, respectively. In addition, when compared the photostability in air with the photostability in nitrogen, the most significant differences were observed for CTAB-Sap/ACN, which corroborate with the greater exposure of ACN molecules to oxygen attack on air atmosphere for these hybrids.

4. Conclusion

It is known that the quinoidal base form of anthocyanin is less stable than the flavylium one and it occurs in neutral to basic conditions. The stabilization of quinoidal base form was brought by the intermolecular interactions in CTAB-Sap/ACN, since the synthesis of the hybrids were performed at pH 3. In the Sap/ACN pigment, a cation exchange mechanism leads to the intercalation of the flavylium cation of the natural dye. The enhanced stability against visible light irradiation and basic environmental conditions was brought by the intercalation and/or the intermolecular interaction between the dye and the respective host materials. The intercalation of the dye molecules into the interlayer space of saponite in Sap/ACN sample provide more protection against reactive oxygen species. Reversibility in color upon exposure to acidic and basic atmosphere is an evidence for a possible application of the obtained pigments as a sensor to atmospheric acidity, which can be exploited in several cycles if applied in less extreme pH conditions. These dyed materials are environmentally friendly and can be promising candidates in different application fields.

Declaration of Competing Interest.

The authors declare that they have no known competing financial interests or personal relationships that could have appeared to influence the work reported in this paper

Acknowledgment

We acknowledge the financial support from the CAPES/COFEBUB (Project No. 835/15), CAPES and National Council for Scientific and Technological Development (CNPq, Brazil) for financial support (Grant 310921/2017-1, M.G.F, 307460/2016-9, E.C.S.F.). The authors thank the Île-de-France region and CNRS for funding.

REFERENCES

Baez, E., Quazi, N., Ivanov, I., Bhattacharya, S.N., 2009. Stability study of nanopigment dispersions. Adv. Powder Technol. 20, 267–272. https://doi.org/10.1016/j.apt.2009.02.005

Brouillard, R., 1982. Chemical Structure of Anthocyanins, in: Markakis, P. (Ed.), Anthocyanins As Food Colors. Academic Press, pp. 1–40. https://doi.org/10.1016/b978-0-12-472550-8.50005-6

Chen, H., Zhang, Z., Zhuang, G., Jiang, R., 2019. A new method to prepare 'Maya red' pigment from sepiolite and Basic red 46. Appl. Clay Sci. 174, 38–46. https://doi.org/10.1016/j.clay.2019.03.023

De Queiroga, L.N.F., França, D.B., Rodrigues, F., Santos, I.M.G., Fonseca, M.G., Jaber, M., 2019. Functionalized bentonites for dye adsorption: Depollution and production of new pigments. J. Environ. Chem. Eng. 7, 103333. https://doi.org/10.1016/j.jece.2019.103333

Eskandarabadi, S.M., Mahmoudian, M., Farah, K.R., Abdali, A., Nozad, E., Enayati, M., 2019. Active intelligent packaging film based on ethylene vinyl acetate nanocomposite containing extracted anthocyanin, rosemary extract and ZnO/Fe-MMT nanoparticles. Food Packag. Shelf Life 22, 100389. https://doi.org/10.1016/j.fpsl.2019.100389

Fang, J.-L., Luo, Y., Yuan, K., Guo, Y., Jin, S.-H., 2020. Preparation and evaluation of an encapsulated anthocyanin complex for enhancing the stability of anthocyanin. LWT - Food Sci. Technol. 117, 1–8. https://doi.org/10.1016/J.LWT.2019.108543

Fatimah, I., Rubiyanto, D., Prakoso, N.I., Yahya, A., Sim, Y.-L., 2019. Green conversion of citral and citronellal using tris(bipyridine)ruthenium(II)-supported saponite catalyst under microwave irradiation. Sustain. Chem. Pharm. 11, 61–70. https://doi.org/10.1016/J.SCP.2019.01.001

Jaber, M., Miéhé-Brendlé, J., 2005. Influence du milieu de synthése sur la cristallisation de saponite: Proposition de mécanisme réactionnel en milieux acide et basique. Comptes Rendus Chim. 8, 229–234. https://doi.org/10.1016/j.crci.2004.10.025

Kohno, Y., Kinoshita, R., Ikoma, S., Yoda, K., Shibata, M., Matsushima, R., Tomita, Y., Maeda, Y., Kobayashi, K., 2009. Stabilization of natural anthocyanin by intercalation into montmorillonite. Appl. Clay Sci. 42, 519–523. https://doi.org/10.1016/j.clay.2008.06.012

Koosha, M., Hamedi, S., 2019. Intelligent Chitosan/PVA nanocomposite films containing black carrot anthocyanin and bentonite nanoclays with improved mechanical, thermal and antibacterial properties. Prog. Org. Coatings 127, 338–347. https://doi.org/10.1016/J.PORGCOAT.2018.11.028

Li, S., Ding, J., Mu, B., Wang, X., Kang, Y., Wang, A., 2019a. Acid/base reversible allochroic anthocyanin/palygorskite hybrid pigments: Preparation, stability and potential applications. Dye. Pigment. 171, 107738. https://doi.org/10.1016/J.DYEPIG.2019.107738

Li, S., Mu, B., Wang, X., Kang, Y., Wang, A., 2019b. A comparative study on color stability of anthocyanin hybrid pigments derived from 1D and 2D clay minerals. Materials (Basel). 12, 1–14. https://doi.org/10.3390/ma12203287

Lu, Y., Dong, W., Wang, W., Wang, Q., Hui, A., Wang, A., 2019. A comparative study of different natural palygorskite clays for fabricating cost-efficient and eco-friendly iron red composite pigments. Appl. Clay Sci. 167, 50–59. https://doi.org/10.1016/j.clay.2018.10.008

Marçal, L., De Faria, E.H., Nassar, E.J., Trujillano, R., Martín, N., Vicente, M.A., Rives, V., Gil, A., Korili, S.A., Ciuffi, K.J., 2015. Organically Modified Saponites: SAXS Study of Swelling and Application in Caffeine Removal. ACS Appl. Mater. Interfaces 7, 10853–10862. https://doi.org/10.1021/acsami.5b01894

318 Micó-Vicent, B., López-Herraiz, M., Bello, A., Martínez, N., Martínez-Verdú, F.M., 2017.
319 Synthesis of pillared clays from metallic salts as pigments for thermosolar absorptive
320 coatings. Sol. Energy 155, 314–322. https://doi.org/10.1016/j.solener.2017.06.034

321 Ogawa, M., Takee, R., Okabe, Y., Seki, Y., 2017. Bio-geo hybrid pigment; clay-anthocyanin
322 complex which changes color depending on the atmosphere. Dye. Pigment. 139, 561–565.
323 https://doi.org/10.1016/J.DYEPIG.2016.12.054

324 Piffaut, B., Kader, F., Girardin, M., Metche, M., 1994. Comparative degradation pathways of
325 malvidin 3,5-diglucoside after enzymatic and thermal treatments. Food Chem. 50, 115–120.
326 https://doi.org/10.1016/0308-8146(94)90106-6

327 Pimchan, P., Khaorapapong, N., Ogawa, M., 2014. The effect of cetyltrimethylammonium ion
328 and type of smectites on the luminescence efficiency of bis(8-hydroxyquinoline)zinc(II)
329 complex. Appl. Clay Sci. 101, 223–228. https://doi.org/10.1016/J.CLAY.2014.08.004

330 Samuei, S., Rad, F.A., Rezvani, Z., 2020. The influence of intercalated dye molecules shape and
331 features on photostability and thermal stability between LDH layers. Appl. Clay Sci. 184,
332 105388. https://doi.org/10.1016/j.clay.2019.105388

333 Silva, F. de C., Lima, L.C.B., Silva-Filho, E.C., Fonseca, M.G., Jaber, M., 2020. Through
334 alizarin-hectorite pigments: Influence of organofunctionalization on fading. Colloids
335 Surfaces A Physicochem. Eng. Asp. 587, 124323.
336 https://doi.org/10.1016/J.COLSURFA.2019.124323

337 Silva, G.T.M., Silva, C.P., Gehlen, M.H., Oake, J., Bohne, C., Quina, F.H., 2018.
338 Organic/inorganic hybrid pigments from flavylium cations and palygorskite. Appl. Clay
339 Sci. 162, 478–486. https://doi.org/10.1016/j.clay.2018.07.002

340 Tangaraj, V., Janot, J.-M., Jaber, M., Bechelany, M., Balme, S., 2017. Adsorption and
341 photophysical properties of fluorescent dyes over montmorillonite and saponite modified by
342 surfactant. Chemosphere 184, 1355–1361.
343 https://doi.org/10.1016/J.CHEMOSPHERE.2017.06.126

344 Tao, Q., Fang, Y., Li, T., Zhang, D., Chen, M., Ji, S., He, H., Komarneni, S., Zhang, H., Dong,

Y., Noh, Y.D., 2016. Silylation of saponite with 3-aminopropyltriethoxysilane. Appl. Clay Sci. 132–133, 133–139. https://doi.org/10.1016/J.CLAY.2016.05.026

Teixeira-Neto, Â.A., Izumi, C.M.S., Temperini, M.L.A., Ferreira, A.M.D.C., Constantino, V.R.L., 2012. Hybrid materials based on smectite clays and nutraceutical anthocyanins from the Açaí fruit. Eur. J. Inorg. Chem. 5411–5420. https://doi.org/10.1002/ejic.201200702

Torres, B., Tiwari, B.K., Patras, A., Cullen, P.J., Brunton, N., O'Donnell, C.P., 2011. Stability of anthocyanins and ascorbic acid of high pressure processed blood orange juice during storage. Innov. Food Sci. Emerg. Technol. 12, 93–97. https://doi.org/10.1016/J.IFSET.2011.01.005

Trigueiro, P., Pereira, F.A.R., Guillermin, D., Rigaud, B., Balme, S., Janot, J.M., dos Santos, I.M.G., Fonseca, M.G., Walter, P., Jaber, M., 2018. When anthraquinone dyes meet pillared montmorillonite: Stability or fading upon exposure to light? Dye. Pigment. 159, 384–394. https://doi.org/10.1016/j.dyepig.2018.06.046

Wang, L., Wang, A., 2008. Adsorption properties of Congo Red from aqueous solution onto surfactant-modified montmorillonite. J. Hazard. Mater. 160, 173–180. https://doi.org/10.1016/j.jhazmat.2008.02.104

Zhang, C., He, H., Tao, Q., Ji, S., Li, S., Ma, L., Su, X., Zhu, J., 2017. Metal occupancy and its influence on thermal stability of synthetic saponites. Appl. Clay Sci. 135, 282–288. https://doi.org/10.1016/J.CLAY.2016.10.006

Zhuang, G., Jaber, M., Rodrigues, F., Rigaud, B., Walter, P., Zhang, Z., 2019a. A new durable pigment with hydrophobic surface based on natural nanotubes and indigo: Interactions and stability. J. Colloid Interface Sci. 552, 204–217. https://doi.org/10.1016/J.JCIS.2019.04.072

Zhuang, G., Rodrigues, F., Zhang, Z., Fonseca, M.G., Walter, P., Jaber, M., 2019b. Dressing protective clothing: stabilizing alizarin/halloysite hybrid pigment and beyond. Dye. Pigment. 166, 32–41. https://doi.org/10.1016/j.dyepig.2019.03.006